5th International Symposium on Three-Dimensional Electromagnetics
Sapporo, Japan, May 7–9, 2013

Three-dimensional transient electromagnetic simulation using Rational Krylov subspace projection methods

Ralph-Uwe Börner[1], Oliver G. Ernst[2], Stefan Güttel[3]
[1]TU Bergakademie Freiberg, Germany, Institute of Geophysics and Geoinformatics
[2]TU Bergakademie Freiberg, Germany, Institute of Numerical Analysis and Optimization
[3] University of Manchester, UK, School of Mathematics

SUMMARY

The rapid inversion of 3-D electromagnetic (EM) measurements to obtain maps of the electrical conductivity of subsurface regions of interest remains one of the major computational challenges of geoelectromagnetic prospecting. The forward simulation step, in which the response of a given conductivity distribution is computed, remains a key element in the inversion process, since it must be carried out multiple times for each inversion. The availability of fast forward modelling codes is therefore of crucial importance.

The discretization of Maxwell's equations in the time and frequency domain yields linear algebra problems that can be formulated in terms of matrix functions $f^\tau(\boldsymbol{A})\boldsymbol{b}$ with $f^\tau(z) = \exp(\tau z)$ and $f^\tau(z) = (z-\tau)^{-1}$, respectively. In our application, where the problem size N is very large, it is not possible to compute the dense matrix $f^\tau(\boldsymbol{A})$ explicitly.

We will consider approximation methods for these matrix functions, which avoid the computation of large matrix functions and directly compute approximations to the vector $f^\tau(\boldsymbol{A})\boldsymbol{b}$ by projection on low-dimensional subspaces.

We will show numerical examples and compare our results in terms of numerical accuracy and efficiency.

Keywords: forward modeling, time-domain, finite elements, Krylov subspace method

INTRODUCTION

Time-domain electromagnetic methods (TEM) for geophysical exploration attempt to reconstruct the distribution of subsurface conductivity from measurements of the Earth's transient electromagnetic response to artificial sources. Such a reconstruction entails the numerical solution of a challenging large-scale parameter estimation problem involving the solution of a sequence of initial-boundary value problems for the quasi-static Maxwell's equations, the so-called *forward modelling* step.

Aside from methods based on integral equations, there are several options for solving the time-dependent PDE based on a given spatial discretization. The most immediate is time-stepping, i.e., approximating the solution of the semi-discretized problem by numerical methods for systems of ODEs. Due to the parabolic nature of the governing equations only unconditionally stable time-stepping methods are practical due to the otherwise excessively small time-steps necessary.

A broad distinction in TEM forward modelling schemes is between *time domain* and *frequency domain* methods. In the first, the time evolution of electromagnetic fields is propagated forward in time, whereas in the latter the Fourier components of these fields are computed for a suitable collection of frequencies, which are then transformed numerically to the time domain (Börner et al., 2008).

GOVERNING EQUATIONS

Neglecting displacement currents, the time-dependent Maxwell's equations for the electric field intensity $\boldsymbol{e} = \boldsymbol{e}(\boldsymbol{x},t)$ and magnetic field intensity $\boldsymbol{h} = \boldsymbol{h}(\boldsymbol{x},t)$ at location $\boldsymbol{x} = [x,y,z]^\top$ and time t are given by

$$\begin{aligned} \nabla\times\boldsymbol{e} + \mu\partial_t\boldsymbol{h} &= \boldsymbol{0}, \\ \nabla\times\boldsymbol{h} - \sigma\boldsymbol{e} &= \boldsymbol{j}^e, \\ \nabla\cdot\boldsymbol{h} &= 0, \end{aligned} \tag{1}$$

where $\sigma = \sigma(\boldsymbol{x})$ is the electric conductivity, μ is the magnetic permeability and $\boldsymbol{j}^e = \boldsymbol{j}^e(\boldsymbol{x},t)$ denotes an impressed external source current density. After eliminating $\boldsymbol{h}$ from (1) we obtain the second order partial differential equation

$$\sigma\partial_t\boldsymbol{e} + \nabla\times(\mu^{-1}\nabla\times\boldsymbol{e}) = -\partial_t\boldsymbol{j}^e, \qquad t\in\mathbb{R}, \tag{2}$$

for the electric field. We assume these equations to hold on a computational domain $\Omega\subset\mathbb{R}^3$ containing the air-earth interface and impose the perfect conductor boundary

condition

$$\boldsymbol{n}\times\boldsymbol{e}=\boldsymbol{0} \qquad \text{along } \partial\Omega, \tag{3}$$

where we make the implicit assumption that the boundary $\partial\Omega$ of Ω has been placed at sufficient distance from sources that the effects of the boundary conditions is negligible compared to discretization errors.

We consider a source term $\boldsymbol{j}^e$ resulting from a stationary transmitter with a driving current that is shut off at time $t=0$, giving

$$\boldsymbol{j}^e(\boldsymbol{x},t)=\boldsymbol{q}(\boldsymbol{x})H(-t) \tag{4}$$

in which H denotes the Heaviside unit step function and the vector field $\boldsymbol{q}$ denotes the spatial current pattern. Specifically, we consider a transmitter consisting of a small horizontal square wire-loop carrying a stationary current of given magnitude I, thus generating a good approximation of a vertical magnetic dipole.

The combination of (2), (3) and (4) results in the initial-boundary value problem

$$\sigma\partial_t\boldsymbol{e}+\nabla\times(\mu^{-1}\nabla\times\boldsymbol{e})=-\partial_t\boldsymbol{j}^e \quad \text{on } \Omega, \tag{5a}$$

$$\boldsymbol{e}|_{t=0}=\boldsymbol{q} \quad \text{on } \Omega, \tag{5b}$$

$$\boldsymbol{n}\times\boldsymbol{e}=\boldsymbol{0} \quad \text{along } \partial\Omega \tag{5c}$$

for the electric field $\boldsymbol{e}$ as a function of time and space.

To formulate the same problem in the frequency domain, we apply the Fourier transform in time, denoted by the operator $\mathscr{F}$, to both sides of (2). Introducing the transformed electric field

$$\boldsymbol{E}(\boldsymbol{x},\omega):=(\mathscr{F}\boldsymbol{e})(\omega)=\int_{-\infty}^{\infty}\boldsymbol{e}(\boldsymbol{x},t)\,\mathrm{e}^{-i\omega t}\,\mathrm{d}t, \qquad \omega\in\mathbb{R},$$

observing the the correspondence $(\mathscr{F}H)(\omega)=\pi\delta(\omega)+\frac{1}{i\omega}$, where δ denotes the Dirac delta distribution concentrated at zero, as well as the scaling and derivative laws for the Fourier transform, we obtain the frequency-domain equation

$$\nabla\times(\mu^{-1}\nabla\times\boldsymbol{E})+i\omega\sigma\boldsymbol{E}=-i\omega\boldsymbol{q}\left(\pi\delta(\omega)-\frac{1}{i\omega}\right). \tag{6}$$

To simplify the problem, we introduce the impulse response electric field $\boldsymbol{e}_i=\boldsymbol{e}_i(\boldsymbol{x},t)$ as the solution of (2) with impulsive source current $\boldsymbol{j}_i^e(\boldsymbol{x},t)=\boldsymbol{q}(\boldsymbol{x})\delta(t)$. In view of the relation $(\mathscr{F}\delta)(\omega)\equiv 1$, its Fourier transform $\boldsymbol{E}_i=\boldsymbol{E}_i(\boldsymbol{x},\omega)$ satisfies

$$\nabla\times(\mu^{-1}\nabla\times\boldsymbol{E}_i)+i\omega\sigma\boldsymbol{E}_i=-i\omega\boldsymbol{q}. \tag{7}$$

We remove the frequency-dependence of the right-hand side of (7) by introducing a new dependent vector field $\boldsymbol{A}_i=\boldsymbol{A}_i(\boldsymbol{x},\omega)$ such that $\boldsymbol{E}_i=-i\omega\boldsymbol{A}_i$, which satisfies

$$\nabla\times(\mu^{-1}\nabla\times\boldsymbol{A}_i)+i\omega\sigma\boldsymbol{A}_i=\boldsymbol{q}. \tag{8}$$

We note that the fields $\boldsymbol{E}$, $\boldsymbol{E}_i$ and $\boldsymbol{A}_i$ in equations (6), (7) and (8) satisfy the same homogeneous boundary condition (3) and the same PDE with right-hand sides which are all scalar multiples of $\boldsymbol{q}$, implying

$$\boldsymbol{E}(\omega)=\left(\pi\delta(\omega)-\frac{1}{i\omega}\right)\boldsymbol{E}_i(\omega)=\big(1-i\pi\omega\delta(\omega)\big)\boldsymbol{A}_i(\omega). \tag{9}$$

Transforming back to the time domain results in the transient solutions

$$\begin{aligned}\boldsymbol{e}(\boldsymbol{x},t)&=\frac{1}{2\pi}\int_{-\infty}^{\infty}\boldsymbol{E}(\boldsymbol{x},\omega)\,e^{i\omega t}\,d\omega\\&=\frac{1}{2\pi}\int_{-\infty}^{\infty}\left(\pi\delta(\omega)-\frac{1}{i\omega}\right)\boldsymbol{E}_i(\omega)\,e^{i\omega t}\,d\omega\\&=\frac{1}{2\pi}\int_{-\infty}^{\infty}\Big(1-i\pi\omega\delta(\omega)\Big)\boldsymbol{A}_i(\omega)\,e^{i\omega t}\,d\omega\\&=\frac{1}{2\pi}\int_{-\infty}^{\infty}\boldsymbol{A}_i(\omega)\,e^{i\omega t}\,d\omega, \qquad t\in\mathbb{R}.\end{aligned} \tag{10}$$

DISCRETIZATION IN SPACE

The finite element discretization of (5) reads

$$\boldsymbol{M}\partial_t\boldsymbol{e}+\boldsymbol{C}\boldsymbol{e}=\boldsymbol{0}, \quad \boldsymbol{e}(0)=\boldsymbol{q}, \tag{11}$$

and its explicit solution is given in terms of the matrix exponential function

$$\boldsymbol{e}(t)=f^t(\boldsymbol{A})\boldsymbol{q}=\exp(-t\boldsymbol{A})\boldsymbol{q},$$

with

$$f^t(z)=\exp(-tz), \quad \boldsymbol{A}=\boldsymbol{M}^{-1}\boldsymbol{C}.$$

Similarly, the finite element discretization of the frequency domain problem (8) results in the linear system of equations

$$(\boldsymbol{C}+i\omega\boldsymbol{M})\boldsymbol{u}=\boldsymbol{q}, \tag{12}$$

in which the real symmetric $N\times N$ matrices $\boldsymbol{C}$ and $\boldsymbol{M}$ result from the curl-curl term $[\boldsymbol{C}]_{j,k}=(\mu^{-1}\nabla\times\phi_j,\nabla\times\phi_k)$ and the zero-order term $[\boldsymbol{M}]_{j,k}=(\sigma\phi_j,\phi_k)$ in the variational equation. A simple algebraic manipulation shows that the solution of this problem can formally be written in terms of the transfer matrix function as

$$\boldsymbol{u}=f^\tau(\boldsymbol{A})\boldsymbol{b}=(\boldsymbol{A}-\tau\boldsymbol{I})^{-1}\boldsymbol{b},$$

where

$$f^\tau(z)=(z-\tau)^{-1}, \quad \tau=-i\omega, \quad \boldsymbol{b}=\boldsymbol{M}^{-1}\boldsymbol{q}.$$

The parameters τ are elements of an *imaginary* parameter interval

$$T=-i[\omega_{\min},\omega_{\max}].$$

RATIONAL KRYLOV METHODS

As shown in the previous section, the discretization of Maxwell's equations in the time and frequency domain yields linear algebra problems that can be formulated in terms of matrix functions $f^\tau(\boldsymbol{A})\boldsymbol{b}$ with $f^\tau(z) = \exp(\tau z)$ and $f^\tau(z) = (z-\tau)^{-1}$, respectively. In our application, where the problem size N is very large, it is not possible to compute the dense matrix $f^\tau(\boldsymbol{A})$ explicitly.

In this section we will consider approximation methods for these matrix functions, which avoid the computation of large matrix functions and directly compute approximations to the vector $f^\tau(\boldsymbol{A})\boldsymbol{b}$ by projection on low-dimensional subspaces. These so-called rational Krylov methods all have in common that the function f^τ is replaced by a rational function r_n^τ with known denominator. More precisely, given a fixed polynomial q_{n-1} of degree $n-1$, we will approximate the vector $f^\tau(\boldsymbol{A})\boldsymbol{b}$ by $r_n^\tau(\boldsymbol{A})\boldsymbol{b}$, where the numerator p_{n-1}^τ of the rational function $r_n^\tau = p_{n-1}^\tau / q_{n-1}$ is chosen implicitly by a projection method. The linear space $\mathscr{V}_n$ of all vectors being representable as rational functions with the same denominator q_{n-1} is called a *rational Krylov space* (Ruhe, 1984, 1994),

$$\begin{aligned} \mathscr{V}_n &= \operatorname{span}\left\{ \frac{p_{n-1}}{q_{n-1}}(\boldsymbol{A})\boldsymbol{b} : \deg(p_{n-1}) \le n-1 \right\} \\ q_{n-1}(z) &= \prod_{j=1}^{n-1}(1 - z/\xi_j). \end{aligned} \tag{13}$$

In the following we will assume that $\mathscr{V}_n$ is of full dimension $n = N$. The feasibility of rational Krylov methods is given when a nearby approximation $\boldsymbol{f}_n^\tau \in \mathscr{V}_n$ to $f^\tau(\boldsymbol{A})\boldsymbol{b}$ exists already for $n \ll N$. In order to extract such an approximation, we first compute an orthonormal basis $V_n = [\boldsymbol{v}_1, \ldots, \boldsymbol{v}_n]$ of $\mathscr{V}_n$ by a rational Arnoldi algorithm.

We equivalently reformulate the problem (12) into the following: Find an approximate solution $\widetilde{\boldsymbol{u}}$ for the problem

$$(\boldsymbol{M}^{-1}\boldsymbol{C} + i\omega\boldsymbol{I})\boldsymbol{u} = \boldsymbol{M}^{-1}\boldsymbol{q}. \tag{14}$$

The only reason for this reformulation is to make obvious that the exact solution of (14) is given as a rational function in the variable $\boldsymbol{A} = \boldsymbol{M}^{-1}\boldsymbol{C}$ multiplied by the right-hand side. More precisely, with $\tau = -i\omega$ and $\boldsymbol{b} = \boldsymbol{M}^{-1}\boldsymbol{q}$ we find that (14) is equivalent to

$$(\boldsymbol{A} - \tau\boldsymbol{I})\boldsymbol{u} = \boldsymbol{b},$$

and the exact solution of this problem is given as

$$\boldsymbol{u} = r(\boldsymbol{A})\boldsymbol{b}, \quad r(z) = (z-\tau)^{-1}.$$

POLE SELECTION

We now turn to the selction of the poles ξ_i in (13). For the frequency domain problem (14) we derive an expression for the matrix function

$$r(z) \approx f(z) = \frac{1}{z + i\omega} \tag{15}$$

with nodes interpolating $f(\boldsymbol{A})$ at the (positive) eigenvalues of $\boldsymbol{A}$, i.e.,

$$z \in \Lambda(\boldsymbol{A}) \subset \mathbb{R}_0^+, \tag{16}$$

and a given parameter interval of frequencies

$$0 < \omega_{\min} \le \omega \le \omega_{\max} < \infty. \tag{17}$$

It can be shown that the optimal rate for a rational Krylov subspace method using a single pole cyclically is obtained by placing the single pole at the geometric mean of the parameter interval, i.e., $\xi = \xi_1 = -i\sqrt{\omega_{\min}\omega_{\max}}$ (Güttel, 2013).

We further investigate other selection strategies for the frequency domain problem. Specifically, we consider

- imaginary Zolotarev poles,
- real asymptotically optimal poles on the negative real axis,
- spectrally adapted imaginary poles, and
- spectrally adapted poles on the negative real axis.

We can completely avoid the inverse Fourier transform by solving the initial-value problem directly in time-domain. This amounts to computing

$$\boldsymbol{u}(t) = H(t)\exp(-t\,\boldsymbol{M}^{-1}\boldsymbol{C})\boldsymbol{b}$$

For this task we can use the same rational Krylov space as before, namely the linear space of rational functions $r(\boldsymbol{A})\boldsymbol{b}$ with $\boldsymbol{A} = \boldsymbol{M}^{-1}\boldsymbol{C}$ and $\boldsymbol{b} = \boldsymbol{M}^{-1}\boldsymbol{q}$.

NUMERICAL EXAMPLE

The following numerical example shall demonstrate that the rational Krylov subspace projection method is accurate and efficient. We consider a simple 3-D model test case, for which an analytical reference solution is available. The model is a layered half-space with resistivities $\rho = [100, 30, 100]\ \Omega\cdot m$ and associated layer thicknesses of $h = [100, 30]$ m. As measurement configuration we use a horizontal co-planar loop orientation at $z = 0$. Loop offset is 100 m. For the purpose of a fair numerical comparison, we will however compare to the algebraic solution obtained by solving a sufficient number of large scale problems (12). More specifically, to obtain a transient for $t \in [10^{-6}, 10^{-3}]$ s, it is a requirement of the involved Hankel transform to provide frequency domain solutions for 110 logarithmically equidistant frequencies. Moreover, to be consistent with the usual data, i.e., a voltage induced an a coil, the curl of $\boldsymbol{u}(t)$ is considered, such that the simulated quantity is in fact $\partial_t B_z(t)$.

For the setup of the rational Krylov subspace we use a single pole on the negative real axis. This pole is repeated 40 times. It therefore makes sense to reuse the once computed LU factors for all remaining linear systems.

Fig. 1 shows a comparison of transient responses obtained by different numerical approaches. It is evident that both time-domain and frequency domain Rational Krylov methods produce results which are identical (in the eyeball norm) to the result obtained by inverse Fourier transform of a large number of full-scale frequency domain solutions with 185,700 finite element degrees of freedom. We note, that the analytical solution serves merely as reference. Due to numerical errors associated with spatial discretization of the PDE as well as the rather small dimension of the Krylov space, it would be unrealistic to expect that accurate results.

Table 1 compares computational times required to obtain results of similar accuracy.

Table 1. Comparison of runtimes for two typical methods to obtain a transient solution $\partial_t B_z(t)$ for $t \in [10^{-6}, 10^{-3}]$ s

Method	Runtime in s
Inverse Fourier transform of full algebraic solution, 110 freq's	2.303,7
Setup of Rational Krylov space with 40 poles	83,3
Projection to full dimension after inverse Fourier transform	10,4
Projection to full dimension after direct evaluation in time-domain	0,6

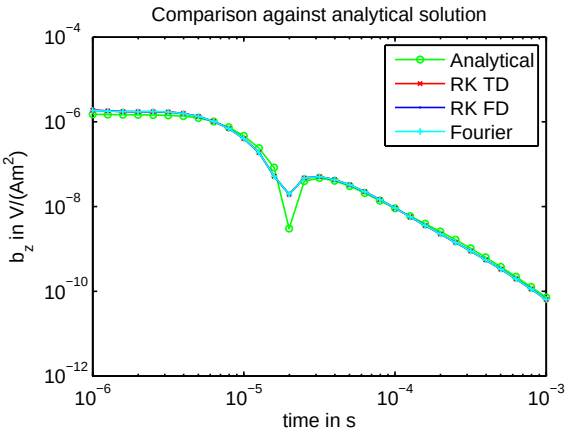

Figure 1. Transient $\partial_t B_z(t)$ for a layered half-space model at $r = 100$ away from a VMD loop source obtained from an analytical solution (Analytical), application of a Rational Krylov method in the frequency domain (RK FD) and time domain (RK TD) as well as inverse Fourier transform of the algebraic frequency domain solution (Fourier).

CONCLUSION

We have presented an effective and accurate method to compute the transient electromagnetic response of a 3-D conductivity distribution. It could be demonstrated that Rational Krylov subspace projection performs far more efficient than the possible (but demanding) alternative approach of transforming a sufficiently large number of full-scale frequency domain solutions back into time-domain.

REFERENCES

Börner, R., Ernst, O. G., & Spitzer, K. (2008). Fast 3D simulation of transient electromagnetic fields by model reduction in the frequency domain using Krylov subspace projection. *Geophys. J. Int.*, *173*, 766–780.

Güttel, S. (2013). Rational Krylov approximation of matrix functions: Numerical methods and optimal pole selection. *GAMM Mitteilungen (to appear)*.

Ruhe, A. (1984). Rational Krylov sequence methods for eigenvalue computation. *Linear Algebra Appl.*, *58*, 391–405. doi: 10.1016/0024-3795(84)90221-0

Ruhe, A. (1994). The rational Krylov algorithm for nonsymmetric eigenvalue problems III: Complex shifts for real matrices. *BIT*, *34*, 165–176.